Raport Badawczy
Research Report

RB/18/2016

Developing a high resolution spatial inventory of GHG emissions for Poland from stationary and mobile sources

R. Bun, Z. Nahorski, J. Horabik-Pyzel,
O. Danylo, L. See, N. Charkovska,
P. Topylko, M. Halushchak, M. Lesiv,
M. Valakh, O. Striamets

Instytut Badań Systemowych
Polska Akademia Nauk

Systems Research Institute
Polish Academy of Sciences

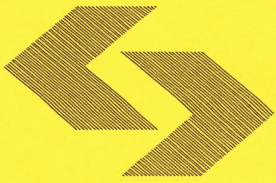

POLSKA AKADEMIA NAUK

Instytut Badań Systemowych

ul. Newelska 6

01-447 Warszawa

tel.: (+48) (22) 3810100

fax: (+48) (22) 3810105

Kierownik Zakładu zgłaszający pracę:
Prof. dr hab. inż. Zbigniew Nahorski

Warszawa 2016

Developing a high resolution spatial inventory of GHG emissions for Poland from stationary and mobile sources

Rostyslav Bun[1,2], Zbigniew Nahorski[3,4], Joanna Horabik-Pyzel[3], Olha Danylo[1,5], Linda See[5], Nadiia Charkovska[1], Petro Topylko[1], Mariia Halushchak[1], Myroslava Lesiv[5], Mariia Valakh[1], Oleksandr Striamets[1]

[1]Lviv Polytechnic National University, Lviv, Ukraine, mail: rbun@org.lviv.net;
[2]Academy of Business in Dąbrowa Górnicza, Poland;
[3]Systems Research Institute of the Polish Academy of Sciences, Warsaw, Poland;
[4]Warsaw School of Information Technology, Warsaw, Poland
[5]International Institute for Applied Systems Analysis, Laxenburg, Austria

Abstract

Greenhouse gas (GHG) inventories at national or provincial levels include the total emissions as well as the emissions for many categories of human activity. The aim of this research was to produce a high resolution spatially explicit emission inventory for these activities for Poland. GHG emission sources are classified into point-, line- and area-types, and then combined to calculate the total emissions. We created vector maps of all sources for all categories of economic activity covered by the IPCC Guidelines, using official information about companies, the administrative maps, Corine Land Cover and other available data. We created the algorithms for disaggregation of these data to the level of elementary objects like the emission sources. We analysed emissions of CO_2, CH_4, N_2O, SO_2, NMVOC, and other greenhouse gases, and we calculated the total emissions in CO_2-equivalent. Gridded data were formulated only at the final stage to present the summarized emissions of very diverse sources from all categories. We considered the grid also as vector map, and what is more the grid cells were split by administrative boundaries into separate objects of vector map. In our approach, the information on administrative assignment of corresponding emission sources is retained, and this makes it possible to aggregate the final results even to the level of municipalities taking into account administrative boundaries unlike traditional gridded emission. In uncertainty analysis we considered uncertainties of the statistical data, of the calorific values, and of the emission factors, with symmetric and asymmetric (lognormal) distributions. On this basis and using Monte-Carlo method, uncertainties expressed as the 95% confidence intervals were estimated for high point-type emission sources, the provinces, and the subsectors.
Keywords: GHG emissions, high resolution spatial inventory, uncertainty, Monte Carlo method

1. Introduction

To counter the impacts of climate change, greenhouse gas (GHG) emissions must be reduced. Reductions can be monitored through inventories of emissions and absorptions of these gases, where national inventory reports are useful for verifying agreed commitments to reduce or stabilize emissions, to estimate the global carbon budget (Le Quéré et al., 2015), to predict the emissions under different scenarios, and to develop and implement new agreements, see e.g. Spencer et al. (2016). GHG inventories at national or provincial levels include data on emissions for many categories of human activity, and the total emissions are calculated using the global warming potential factors of each GHG. The United Nations Framework Convention on Climate Change (UNFCCC), the International Energy Agency (IEA), and the Carbon Dioxide Information Analysis Center (CDIAC) are examples of bodies that collect national inventory submissions and data on emissions broken down by fossil fuel type and by GHG. However, for a more in-depth study of emission processes as well as their structure, it is more appropriate to use spatially explicit data on GHG emissions. Such data link the emissions to the territory in which they appear (Oda and Maksyutov, 2011; Olivier et al., 2005). Thus, they have been used in the past as input data for the simulation of atmospheric CO_2 fluxes in global circulation and transport models (Deque et al., 2012; Neale et al., 2013; Lamarque et al., 2013). Spatially explicit data are also useful for scientists and policy makers at provincial and local levels to identify the main sources of emissions and their structure. Compilation of spatial data is a hot

subject of many recent studies (Andres et al., 2009; Gosh et al., 2010; Gurney et al., 2009; Oda & Maksyutov, 2011; Olivier et al., 2005; Pétron et al., 2008; Puliafito et al., 2015; Raupach et al., 2010; Rayner et al., 2010).

Spatial data on GHG emissions are usually presented in the form of a spatial grid, also referred to as gridded emissions. Emission data at the national or provincial level are disaggregated in order to estimate emissions in each grid cell. These disaggregation algorithms need additional proxy data, e.g. population density. Data from remote sensing can also be used as proxy data, e.g. night-time light intensity, land use data, etc. The disaggregation accuracy can be improved when the emission is significantly correlated in space; see e.g. Horabik & Nahorski (2014). But the final resolution of the gridded emissions is generally determined by the resolution of the proxy data used. Advantages of using remote sensing are the possibility to estimate GHG emissions spatially for large territories (ideally for the whole globe), and the ease of updating emission data over time. These approaches are mainly used for gridded emissions of carbon dioxide (CO_2) as a major GHG produced by humans, which are mainly a result of fossil fuel combustion processes (including emissions by large point sources), land use change and forestry. But there are many categories of anthropogenic activity where emissions cannot be estimated remotely, e.g. emissions of non-methane volatile organic compounds (NMVOCs) or emissions of sulfur hexafluoride (SF_6), which is an extremely potent greenhouse gas, among many others.

Efforts have been made to increase the spatial resolution of the GHG estimates since a higher resolution better reflects the specifics of territorial emission processes (Andres et al., 1996; Oda and Maksyutov, 2011; Olivier et al., 2005; Rayner et al., 2010). Grid cell sizes have decreased from 1° latitude and longitude for global fossil-fuel CO_2 emissions (Andres et al., 2009) to 0.25° (Rayner et al., 2010) and to 1 km for a global fossil fuel CO_2 emission inventory derived using a point source database and satellite observations of night-time lights as proxy data (Oda and Maksyutov, 2011). Spatially explicit GHG emission inventories have also been developed at the regional level, e.g. fossil-fuel CO_2 emissions (Maksyutov et al., 2013; Raupach et al., 2010), fossil fuel combustion CO_2 emission fluxes for the United States (Gurney et al., 2009), as well as data of emission sector or category such as power generation (Pétron et al., 2008), North American methane emissions (Turner et al., 2015), or the road transport sector in Argentina (Puliafito et al., 2015).

There are a number of problems in the practical implementation of GHG gridded emission estimates due to the use of diverse grids for the input proxy data with different spatial resolutions. These may also differ from the desired target resolution of the gridded emissions. When combined, the task is to determine which portion of the grid cell in one grid relates to the partly overlapping cell of the target grid (Verstraete, 2014). These grids can differ in cell size, they can be displaced in any latitude and longitude direction, and they can be even rotated by a certain angle. To address this overlay problem, approaches based on fuzzy control and artificial intelligence techniques can be used (Verstraete 2017). Another problem is that most GHG gridded emission calculations do not fully take into account the state and provincial administrative boundaries, and usually a cell is assigned to an administrative unit based on where the majority of the area falls.

In this paper we propose a completely different approach for estimating a spatially resolved GHG inventory, which is not initially based on a regular grid. Instead we consider emission processes at the level of emission sources, classified into point-, line- and area-type sources. Using data for sources, we created a geospatial database with input parameters and calculated the emissions for each category of human activity using activity data and emission coefficients. The activity data at the level of separate emission sources are calculated using some proxy data and algorithms for disaggregation of the data to the source level, which differs depending on the category of human activity. The digital maps of these emission sources retain information about their administrative assignment; therefore, we can analyze emissions spatially at any administrative level up to municipalities, taking into account administrative boundaries, which

eliminates the problems associated with traditional gridded emission approaches. In the final stage, the emissions from very diverse point-, line-, and area-type sources can be combined to calculate the total emissions in each grid cell, where the target spatial resolution can be very high, e.g. 100m. In this study we analyzed all categories of human activity covered by the IPCC Guidelines (IPCC, 2006) using Poland as a case study. The results include the spatial distribution of not only CO_2, but also other GHGs, as well as the spatial distribution of emissions from different types of fossil fuels. The approach used is very flexible in providing results of many different structural types. The implementation of this approach for the development of a GHG spatial inventory for other sectors, in particular for the electricity generation and fossil fuel processing (Topylko et al., 2017), the residential sector (Danylo et al., 2017), and agriculture (Charkovska et al., 2017) are presented in other papers in this special issue.

2. Methodology and input data

2.1 The spatial GHG inventory approach

The main stages of the proposed approach for creating a GHG spatial inventory are presented in Fig. 1. For all sectors and categories of anthropogenic activity covered by the IPCC Guidelines (IPCC, 2006), the sources of emissions or sinks are analyzed according to their specific features and spatial representation. GHG emission sources are classified into point-, line-, and area-types depending on their emission intensity and physical size as compared to the territory under investigation. These point-, line-, and area-type sources are called 'elementary objects' in our GHG spatial inventory.

Digital maps of emission sources / sinks are built for each category of human activity. For some categories they are digital maps of point objects while for other categories they are digital maps of linear objects or area-type objects. If needed, the line- and area-type (diffused) elementary objects are split by administrative boundaries. This allows us to allocate each elementary object to the corresponding provinces (voivodeships in Poland), districts (powiats) or municipalities (gminas).

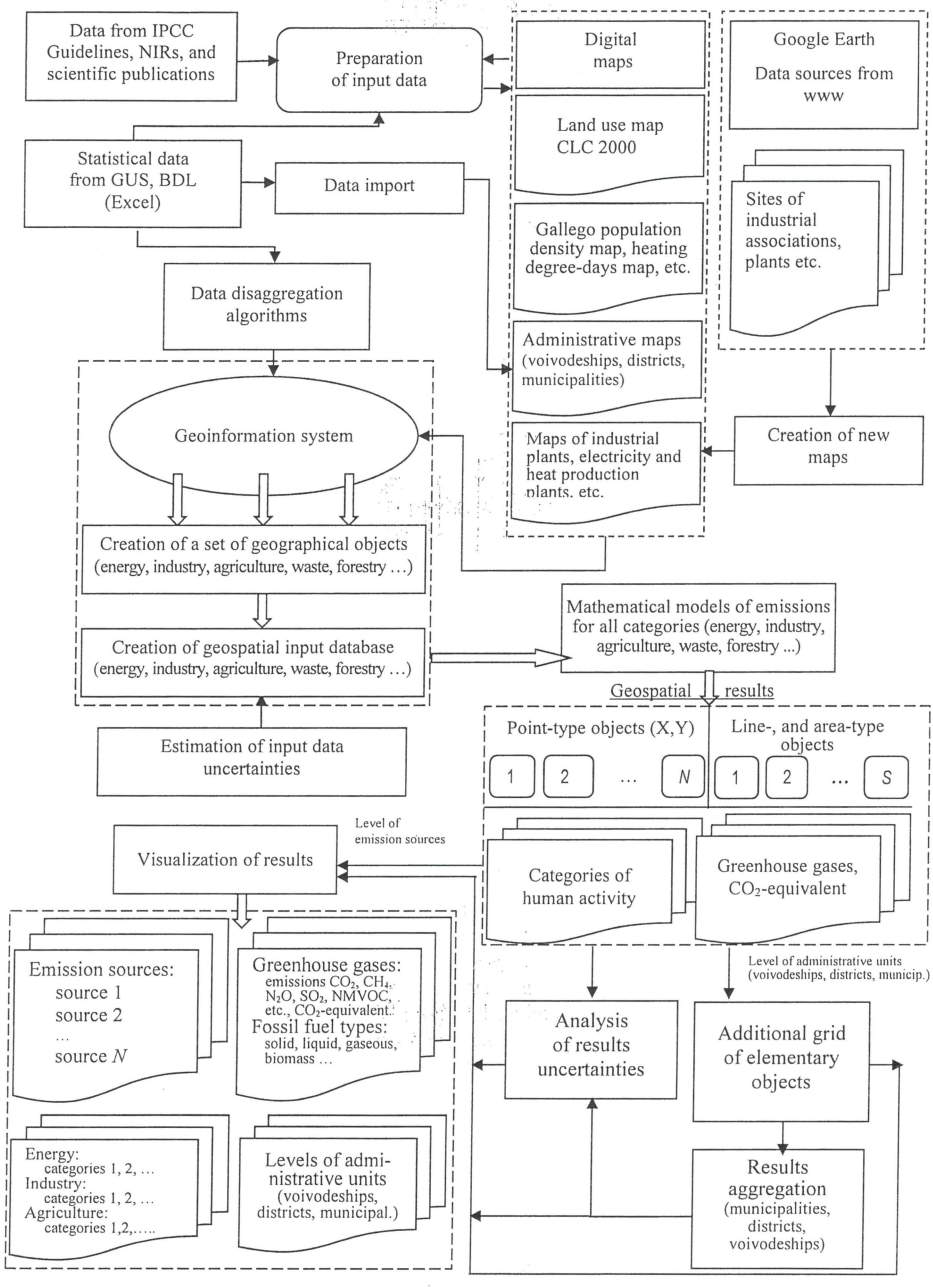

Figure 1. Steps in the development of a GHG spatial inventory

The next step is to calculate GHG emissions from the elementary objects. It reflects the main principles of the IPCC Guidelines (IPCC, 2006), i.e. the emission is a product of the activity data and the corresponding emission factors. However, a common problem is to obtain data about the activities at the level of the elementary objects. For this purpose we have developed algorithms for disaggregation of the available statistical data for provinces (or even for municipalities in some categories) to the level of elementary objects. These algorithms are different for each category of human activity. They take into account the available statistics at the corresponding administrative level, and use other parameters that can be considered as indicators or proxy data for disaggregation of the statistical activity data. We always use the activity / proxy data from the lowest administrative level as a rule.

The unique aspect of this approach to developing a GHG spatial inventory is the ability to use different emission factors for separate elementary objects (or even for parts of objects), if such data are available, as opposed to using averaged or default values employed in more traditional techniques. This approach is extremely relevant for large emission sources such as electricity and heat production plants, iron and steel production, cement production etc. since we can take specific features of technological processes into account such as the applied filters and other equipment as well as the parameters of the fuel used.

In the final stage, the uncertainties of the assessed emissions are estimated using a Monte-Carlo approach with symmetric or asymmetric (lognormal) distributions of the investigated parameters to compute the 95% confidence intervals. This estimation can be applied to the separate emission sources as well as to the aggregated results for the administrative units.

The emissions in each category of the anthropogenic activity for the elementary objects can be visualized in the form of digital maps using different approaches, depending on the source type. The results of the spatial inventory can also be presented separately for each category of emissions, as well as separately for different fossil fuel types or for different GHG.

Since information about the administrative assignment of each elementary object (emission source) is saved in the database, it is possible to aggregate the emissions to administrative units (even for small units like municipalities) without any loss in accuracy as with traditional techniques of gridded emission, when cells of regular grids are used for the estimation of emissions for small territory without taking into account administrative boundaries.

2.2 Input data

2.2.1 High resolution maps of emission sources

As mentioned above, to use the proposed technique for the practical implementation of a GHG spatial inventory, we need high resolution digital maps of very diverse emission sources, which are treated separately as points, lines and areas. Examples of point-type emission sources are electricity or combined electricity and heat production plants, cement plants, production of glass, ammonia, iron and steel, aluminum, pulp and paper, petroleum refining, underground mining etc. (Fig. 2a). Using official information on the addresses of companies in this sector, it is possible to determine the location of their production facilities (i.e. the latitude and longitude) using Google Earth (TM). As the spatial resolution of Google Earth (TM) imagery can be several meters to centimeters, the point-type emission sources are very accurate for the purpose of building the spatial inventory of GHG emissions. Exceptions are when power plants consist of multiple stacks. For example, in the Burshtynska power plant (Ukraine), there are 3 stacks (heights of 250, 250 and 180 meters) with distances of around 100 meters between them. Although we can accurately locate each stack, it is not possible to split the activity data for these stacks so an average location is chosen to represent point sources of this type.

Road and railway transport systems represent examples of line-type emission sources (Fig. 2b). To construct maps of these sources, we used OpenStreetMap (Jokar Arsanjani et al.,

2015), which is a community-based map built through a combination of digitizing very high resolution imagery and paper-based field surveys or with GPS-enabled devices. The spatial resolution of this source of data is also very high. To retain administrative information, roads and railways are additionally split by administrative boundaries into segments, which we consider as separate elementary objects in the inventory. The number of line objects is equal to the number of roads segments. Information on road category is used as one of the indicators for disaggregation of the data on fossil fuel combustion by various categories of vehicle in the transport sector.

Area-type (or diffused) GHG emission sources or sinks are croplands, settlements, industrial areas and forests, among others (Fig. 2c). They consist of a large number of small GHG emission sources / sinks which cannot be regarded separately, but as a whole they can be considered as one emission source / sink within some boundaries. Such area-type objects can be small or large and can be of complicated configuration. In the digital maps, such sources / sinks are represented as polygons for all categories under investigation. The number of such objects is equal to the number of polygons. The objects that correspond to croplands and forests are additionally split by administrative boundaries to retain information on the administrative assignment of the elementary objects. To build these maps, we used Corine Land Cover vector maps (Corine, 2006), which were created from raster maps with a resolution of 100 m. This resolution was used for the digital maps of all area-type sources as well as the final spatial resolution of the GHG spatial inventory.

Note that all point-, line-, and area-type sources are treated as vector digital maps, not raster, in order to retain fully the administrative assignment of each object (even at municipality level), and we use this information for the aggregation of emissions to the corresponding administrative units.

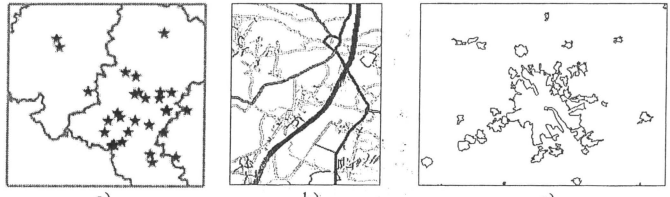

a) b) c)

Figure 2. Examples of emission sources for the GHG spatial inventory: (a) electricity generation plants as point-type sources, (b) roads as line-type sources, and (c) settlements as area-type sources.

2.2.2 Statistical data for Poland and other proxy data

The GHG spatial inventory for Poland covers an area of 312,679 km^2, 16 voivodeships/provinces, 379 powiats/districts and 2,478 gminas/municipalities. We downloaded activity data for different emission categories by province, district and municipality (where available) from the Central Statistical Office of Poland (GUS, 2016) and the Local Data Bank (BDL, 2016). Examples include the amount of fossil fuels used, data about production, number of animals in agriculture, all of which are listed in Table 1. Average national emission factors and the activity data at the national scale were obtained from Poland's National Inventory Report (NIR, 2012).

We also used proxy data for disaggregation of the activity data to the level of elementary objects. Examples of such proxy data are the power of the electricity generation plants (Topylko et al., 2017), population density, data on access to energy sources and the heating degree-days in the residential sector (Danylo et al., 2017), the gross value production in the industry sector

(Charkovska et al., 2017), car numbers and road categories in the road transport sector. The full list is provided in Table 2.

In those cases where it was possible, the emission coefficients and parameters that reflect the territorial specificity of the emission and absorption processes were applied in the emissions calculation. For example, when calculating the accumulated carbon in forests, we used the information from the Local Data Bank (BDL, 2016) on the species composition, the age structure, etc. at the level of districts/powiats and municipalities/gminas.

3. Results

3.1 The spatially explicit GHG inventory for Poland

Using the digital maps of the GHG emission sources / sinks in Poland and the algorithms for activity data disaggregation, a geospatial database was created. The GHG emissions / absorptions were then estimated using appropriate mathematical models. We used disaggregation algorithms and mathematical models of emission processes from the literature to create the GHG spatial inventory as follows:

- for fossil fuel usage (Boychuk et al., 2014), for electricity and heat production (Topylko et al., 2017), for the transport categories (Boychuk et al., 2012; Valakh et al., 2015), for the residential sector (Danylo et al., 2017), and for industry (Halushchak et al., 2016);
- for emissions from fossil fuel extraction and processing (Halushchak et al., 2015);
- for the industrial, agricultural and waste sectors (Charkovska et al., 2017);
- for forestry and land use change (Striamets et al., 2014).

The total emissions in CO_2-equivalents were then calculated for each elementary object using the global warming coefficients, to aggregate the separate emissions. These results were obtained at the level of elementary objects, i.e. point-, line- and area-type sources of emissions. As an example, the total GHG emissions in the transport sector by road type for one Polish province are presented in Fig. 3.

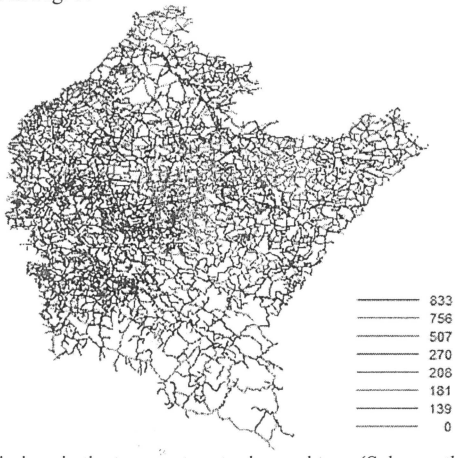

Figure 3. Total GHG emissions in the transport sector by road type (Subcarpathian province, t/km^2, CO_2-equivalent, 2010). (1) national, (2) province/voivodeship, (etc.) district or community roads; and the following road types: highway, express route, dual carriageway, express carriageway, dual carriageway for heavy traffic up to 11.5 t per axle, single carriageway for heavy traffic up to 11.5 t per axle, dual carriageway for heavy traffic up to 10 t per axle, single carriageway for heavy traffic up to 10 t per

axle, dual carriageway up to 8 t per axle, single carriageway up to 8 t per axle, dual carriageway, single carriageway, other with paved surface, dirt road and city road

To calculate these emissions, we took into account the road categories, as specified in Fig. 3. We analyzed the following types of vehicles: scooters, motorcycles, cars, buses and priority vehicles, and used the traffic intensity factors established by experts for these vehicles (Valakh et al., 2015). On this basis, we calculated the amount of gasoline, diesel and liquefied petroleum gas (LPG) used by different types of vehicles on each segment of the road. Then we calculated the emissions of the carbon dioxide CO_2, methane CH_4, and nitrous oxide N_2O from burning gasoline, diesel and LPG, separately, for all types of vehicles and for each road segment. Using the global warming potentials of each GHG, we calculated the total emissions from each road segment.

Similar calculations of GHG emissions were done for all categories of anthropogenic emissions considered here. In the result, the spatial distributions of the GHG emissions (separately for the different gases as well as the total) at the level of the point-, line-, and area-type emission sources were obtained. These data for each category of emissions can be downloaded from www.wwwwww {*this link will be specified*}.

In the final stage, the point-, line-, and area-types emission sources for each emission category summed to calculate the total emissions. In order to do this, we overlaid a grid on top of the vector layers where each grid cell is represented as a polygon feature. The grid cells were then split by administrative boundaries into separate elementary objects as shown in Figure 4 so that each grid cell retains information about the corresponding administrative units. For example, in the central cell in the lowest level the road crosses the administrative boundary. Hence, it is assigned in this cell partly to the administrative unit in the left side of the cell (area 17), and partly to the unit in the right side (area 18). In this way, the total emissions from all categories can be calculated. Any grid size can be chosen as long as it is larger than 100 m due to the limit of the data used to derive the area-type emission sources. However, for visualization purposes, we used a 2 km grid size for calculating the emissions.

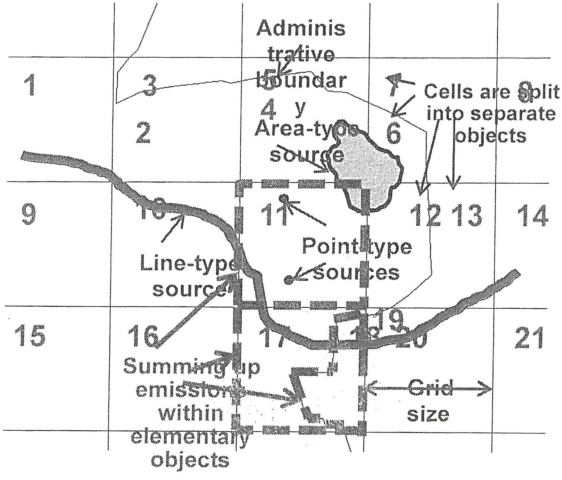

Figure 4. Combining diverse GHG emission sources into a grid where the cells are split by administrative boundaries into separate elementary objects of the vector map.

Figure 5 provides a map of the total GHG emissions for all categories of the energy, industry, agriculture and waste sectors for Poland and for the Silesian voivodeship, which is the most industrialized Polish province. An alternative representation is provided in Figure 6 for the Silesian province in Poland using a prism map and the square root of the emissions for better visualization of the results. For the purpose of visualization, the results have been aggregated to a regular 2 km grid although the data are available at a spatial resolution of 100 m.

As mentioned previously, the total emissions can be calculated for any administrative unit at the level of gmina/municipality, powiat/district or voivodeship/province without any loss of accuracy. Figure 7 shows the total GHG emissions by sector in Poland at a provincial level while Figure 8 focuses on emissions in the energy sector, which has the largest influence on total emissions.

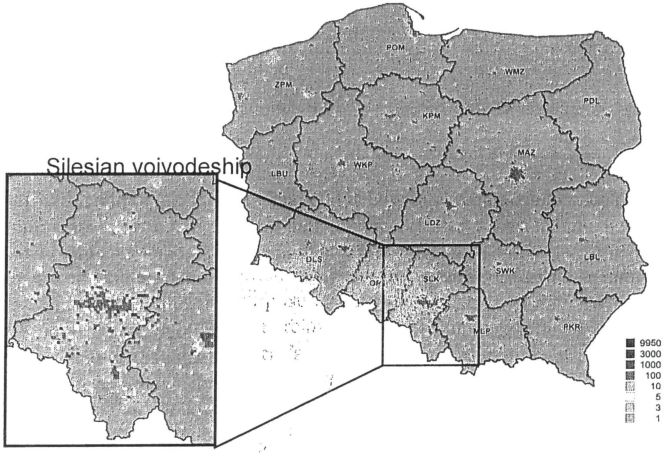

Figure 5. Total GHG emissions in Poland and for the Silesian province (all categories without LULUCF, 2010, Gg/cell area, CO_2-equivalent, 2 km grid size)

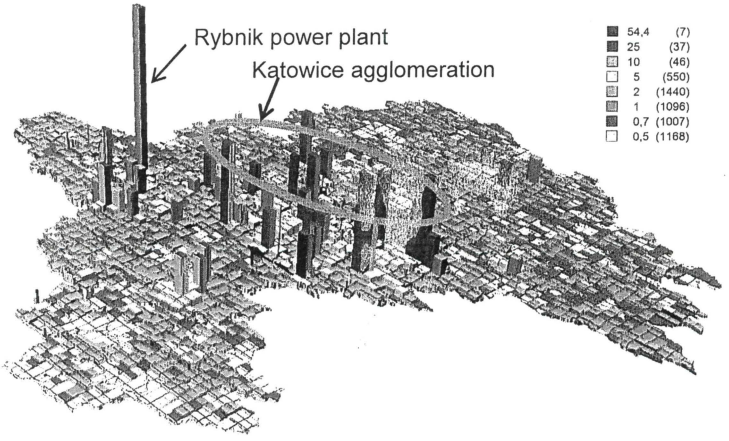

Figure 6. Prism-map of specific GHG emissions from all sectors/categories of human activity without LULUCF in Silesia province at the level of elementary objects (CO_2-equivalent, Gg/km^2, square root scale, 2 x 2 km, 2010)

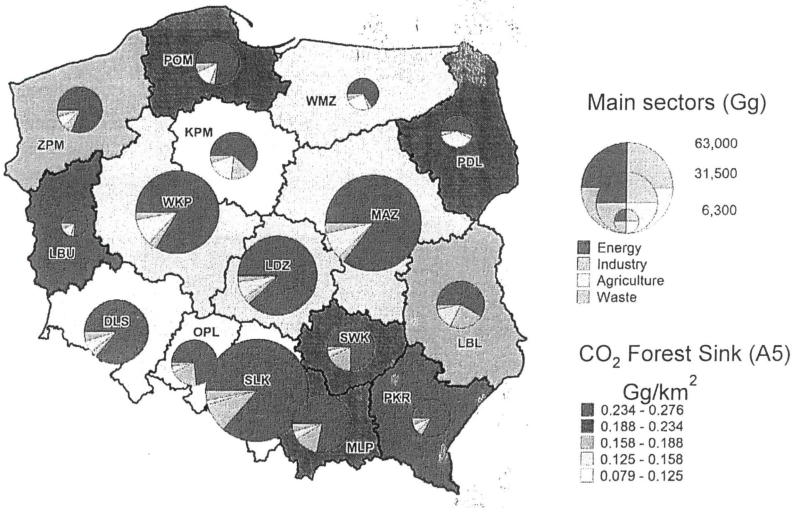

Figure 7. Total GHG emissions by province and sector (Poland, CO_2-equivalent, 2010)

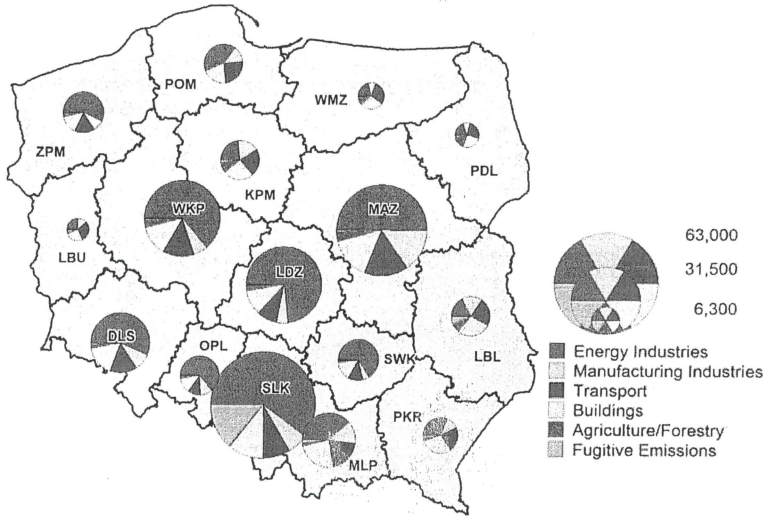

Figure 8. Total GHG emissions in the energy sector by province and sub-sector (Poland, Gg, CO_2-equivalent, 2010)

3.2 Uncertainty analysis

The variables and parameters used in the GHG inventory are often highly uncertain (IPCC, 2001). These uncertainties are associated with a lack of knowledge about emission processes, inaccurate measuring instruments, etc. (Ometto, 2015; White, 2011). There are a number of potential uncertainties in the GHG spatial inventory produced here, which can arise from the following factors:

a) uncertainty in the geolocation of emission sources and sinks;
b) uncertainty in the aggregated activity / statistical data;
c) uncertainty in the proxy data representation (uncertainty in the spatial disaggregation of the activity data to the level of the elementary objects using disaggregation algorithms and disaggregation coefficients on the basis of some indicators or proxy data);
d) uncertainty in the proxy data values;
e) uncertainty in the proxy data geolocation;
f) uncertainty in the emission factors.

When preparing gridded emissions in a bigger regions, the accuracy of the geolocation of sources plays a key role in the uncertainty of the results (Oda et al., 2017). However, this factor is not considered in this study because the uncertainty in locating the point- and line-type elementary objects is small, especially for big emission sources since we used Google Earth (TM) and visual inspection of the sources. We created vector maps of emission sources and determined their geographical coordinates very precisely instead of using a raster grid employed in other approaches. Only power plants with multiple stacks make some problems, as we model such group of stacks as one stack with average parameters. This introduces an uncertainty in the geolocation but is neglected in this study. The uncertainty in the location of the area-type (diffused) emission sources / sinks is a function of the minimum mapping unit of the Corine Land Cover maps (Corine, 2006), which is 100 m, and the accuracy of this product which is x%.

Regarding the uncertainty of the input statistical data such as the uncertainty of the calorific values or emission factors, data from various sources (IPCC, 2001; NIR, 2012; GUS, 2016) and other studies (e.g. Hamal 2009) have been used. For these variables, we used symmetric and asymmetric (lognormal) distributions, and 95% confidence intervals.

As described above, the algorithms for disaggregation of the activity data are based on certain proxies, the values of which were mostly fixed using statistical data. Therefore, it was assumed that the uncertainties in the proxy data values are the same as for the statistical data used. For some categories of human activities, such as in the residential sector, the uncertainties of disaggregated data were evaluated by comparison with similar data from other known sources (GUS, 2016; BDL, 2016). These results are presented in a number of different studies (Topylko et al., 2017; Danylo et al., 2017; Halushchak et al., 2016; Halushchak et al., 2015; Charkovska et al., 2017).

Based on these input uncertainties, we estimated the distributions of the emissions using the Monte-Carlo method as the mean value and the lower and upper limits of the 95% confidence intervals. For point-type sources, we estimated the uncertainty of the results separately for each source. We also analyzed the sensitivity of the total uncertainty to changes in the separate component uncertainties such as the statistical data, the calorific values and the emission factors. These results are presented in a number of papers (Topylko et al., 2017; Danylo et al., 2017; Halushchak et al., 2016; Halushchak et al., 2015; Charkovska et al., 2017).

As the number of elementary objects for line- and area-type sources are large (typically tens of thousands, as in the residential or agriculture sectors), we also evaluated the uncertainties of the results and their sensitivity to changes in the uncertainties of the separate components using the Monte-Carlo method, but at the province level.

The influence of the above mentioned factors were analyzed separately. For the combined investigation of the factors, the approach presented in Hogue et al. (2017) can be applied. The

learning process outlined in Jonas et al. (2017) can be used for the continual improvement of GHG emission inventories and uncertainties.

4. Discussion and Conclusions

The approach presented in this paper results in a high resolution GHG spatial inventory composed of point-, line-, and area-type emission sources / sinks. The spatial analysis is carried out directly at the level of these sources as vector features in contrast to more traditional grid-based emission approaches. Consequently, information on the administrative assignment of corresponding emission sources (plants, settlements, road segments, croplands, etc.) is retained, and this, in turn, makes it possible to aggregate the final results to different sub-national levels, even down to sub-municipalities without decreasing the accuracy of results. The approach also enables the display and analysis of contributions from all territories, even very small ones, to the overall emission process. This approach also allows for the production of a GHG spatial inventory for all categories of human activities, for all GHGs and for all fossil fuel types separately, which is important for the analysis of emissions by sector and the subsequent effectiveness of local decision making on emission reductions. Moreover, each value from traditional national inventory reports can be represented spatially. Such an inventory provides a considerable amount of new knowledge about emission processes, which may be very useful for decision makers and scientists.

In principle, according to this approach, the spatial inventory of the GHG emissions is carried out by the 'bottom-up' method, but there exist in it also elements of the 'top-down' assessment, since we disaggregate the available statistical or proxy data to the level of elementary objects, that is the point-, line-, or area-type sources of the GHG emissions / sinks. Therefore, this technique can be classified as a hybrid approach to forming the GHG spatial inventory. However, the approach makes it possible to fully use the available, even partial information about the territorial specificity of the emission or absorption processes, especially the specific features of the fossil fuels used, and the local technological parameters.

The results of the spatial inventory of the GHG emissions / absorption for Poland demonstrate an unevenness of these processes, like very high emissions in the industrial Silesian region and low emissions in the strongly forested Masuria Lakes district. Such an unevenness is typical for many categories of anthropogenic activity. A positive aspect of this is, that the spatial inventory enables displaying a real contribution of each territory to the overall emission processes. The results presented in this form show the emission values and their structural features, which are of interest to authorities to support well-grounded decision making.

Since the spatial analysis takes into account the territorial specificity of many parameters that affect emissions or removals of the greenhouse gases (e.g. the differentiated characteristics of the fossil fuel used in the energy sector, the climatic conditions and the energy sources availability in the residential sector, the species and age composition of forests, and many others), the total inventory for the province/country as a whole becomes more precise than the traditional inventory at the national level, which do not take into account any spatial components and province specificity. Moreover, traditional inventories at the country level are useless for any local analysis. To give an example, high spatial resolutions is needed in modelling local dispersion of emitted gases that enables comparison of their atmospheric concentration with measurements., that can be used for analysis of reliability of the inventory data.

Estimation of uncertainties of the GHG spatial inventories is a complicated task, because it requires examination of influences of many factors, like uncertainty of the emission sources geolocation, uncertainty of the aggregated activity / statistical data, uncertainty of the proxy data representation, uncertainty of both these data values and their geolocation, and uncertainty of the emission factors. Due to well inspected data, in the proposed approach some of these

uncertainties are kept smaller in comparison of other studies, particularly the uncertainties connected with location of big point-type emission sources.

Acknowledgement

The study was conducted within the European Union FP7 Marie Curie Actions IRSES project No. 247645, acronym GESAPU.

References

Andres R.J., Boden T.A., and Marland G. (2009) Annual fossil-fuel CO_2 emissions: Mass of emissions gridded by one degree latitude by one degree longitude, doi:10.3334/CDIAC/ffe.ndp058.2009, 2009.

Andres R.J., Marland G., Fung I., and Matthews E. (1996) A 1° × 1° distribution of carbon dioxide emissions from fossil fuel consumption and cement manufacture, 1950–1990, Global Biogeochem. Cycles, 10(3), 419-429.

BDL 2016 Bank Danych Lokalnych (Local Data Bank), GUS, Warsaw, Poland, Available at: http://stat.gov.pl/bdl.

Boychuk Kh., Bun R. (2014) Regional spatial inventories (cadastres) of GHG emissions in the Energy sector: Accounting for uncertainty, Climatic Change, vol. 124, is. 3, pp. 561-574.

Boychuk P., Nahorski Z., Boychuk Kh., Horabik J. (2012) Spatial analysis of greenhouse gas emissions in road transport of Poland, Econtechmod, vol. 1, is. 4, pp. 9-15.

Charkovska N., Horabik-Pyzel J., Bun R., Danylo O., Nahorski Z., and Jonas M. (2017) Spatial distribution and associated uncertainties of GHG emissions from agriculture sector (this issue).

Corine (2006) Corine Land Cover data, available at: http://www.eea.europa.eu/

Danylo O., Bun R., See L., Topylko P., Xiangyang X., Charkovska N., and Tymków P. (2017) Accounting uncertainty for spatial modeling of greenhouse gas emissions in the residential sector: fuel combustion and heat production (this issue).

Déqué M., Somot S., Sanchez-Gomez E., Goodess C.M., Jacob D., Lenderink G., and Christensen O.B. (2012) The spread amongst ENSEMBLES regional scenarios: regional climate models, driving general circulation models and interannual variability, Climate Dynamics, Vol. 38, Is. 5, 951-964.

Gosh T., Elvidge C.D., Sutton P.C., Baugh K.E., Ziskin D., and Tuttle B.T. (2010) Creating a global grid of distributed fossil fuel CO_2 emissions from nighttime satellite imaginary. Energies, vol. 3, 1895-1913.

Gurney K.R., Mendoza D.L., Zhou Y., Fischer M.L., Miller C.C., Geethakumar S., and de la Rue du Can S. (2009) High resolution fossil fuel combustion CO_2 emission fluxes for the United States, Environ. Sci. Technol., vol. 43, pp. 5535–5541.

GUS 2016 Głuwny Urząd Statystyczny (Central Statistical Office of Poland), Available at: http://stat.gov.pl/en/

Halushchak M., Bun R., Jonas M., Topylko P. (2015) Spatial inventory of GHG emissions from fossil fuels extraction and processing: An uncertainty analysis, Proceedings of the 4th International Workshop on Uncertainty in Atmospheric Emissions, Warsaw, SRI PAS, pp. 64-70.

Halushchak M., Bun R., Shpak N., Valakh M. (2016) Modeling and spatial analysis of greenhouse gas emissions from fuel combustion in the industry sector in Poland, Econtechmod, Vol. 5, Is. 1, pp. 19-26.

Hamal Kh (2009) Geoinformation technology for spatial analysis of greenhouse gas emissions in Energy sector. PhD thesis, Lviv Polytechnic National University, 246 p.

Hogue S., Marland E., and Marland G. (2015) The dependence of uncertainty on scale in gridded data on anthropogenic CO_2 emissions (this issue).

Horabik J., and Nahorski Z. (2014) Improving resolution of a spatial inventory with a statistical inference approach, Climatic Change, Vol. 124, No. 3, pp. 575–589.

IPCC (2006) IPCC Guidelines for National Greenhouse Gas Inventories, Prepared by the National Greenhouse Gas Inventories Programme, Eggleston HS, Buendia L, Miwa K, Ngara T, Tanabe K (eds).

IPCC (2001) Good Practice Guidance and Uncertainty Management in National Greenhouse Gas Inventories, Penman Jim, Dina Kruger, Ian Galbally, Taka Hiraishi, Buruhani Nyenzi, Sal Emmanuel, Lenadro Buendia, Robert Hoppaus, Thomas Martinsen, Jeroen Meijer, Kyoko Miwa and Kiyoko Tanabe.

Jokar Arsanjani, J. Zipf, A. Mooney, P. Helbich, Eds. (2015) OpenStreetMap in GIScience. Lecture Notes in Geoinformation and Cartography. Springer.

Jonas M., Rovenskaya E., Żebrowski P. (2017) Advanced learning from the past to provide a metric for the explainable outreach of historical data (this issue).

Lamarque J. F., Shindell D.T., Josse B., Young P., Cionni I., Eyring V., Bergmann D., Cameron-Smith Ph., Collins W.J., Doherty R.M., Dalsoren S.B., Faluvegi G., Folberth G., Ghan S., Horowitz L.W., Lee Y., MacKenzie I.A., Nagashima T., Naik V., Plummer D.A., Righi M., Rumbold S., Schulz M., Skeie R., Stevenson D.S., Strode S., Sudo K., Szopa S., Voulgarakis A., Zeng G. (2013) The Atmospheric Chemistry and Climate Model Intercomparison Project (ACCMIP): Overview and description of models, simulations and climate diagnostics, Geoscientific Model Development, 6 (1), pp. 179-206.

Le Quéré C., Moriarty R., Andrew R.M., Canadell J.G., Sitch S., Korsbakken J.I., Friedlingstein P., Peters G.P., Andres R.J., Boden T.A., Houghton R.A., House J.I., Keeling R.F., Tans P., Arneth A., Bakker D.C.E., Barbero L., Bopp L., Chang J., Chevallier F., Chini L.P., Ciais P., Fader M., Feely R.A., Gkritzalis T., Harris I., Hauck J., Ilyina T., Jain A.K., Kato E., Kitidis V., Klein Goldewijk K., Koven C., Landschützer P., Lauvset S.K., Lefèvre N., Lenton A., Lima I.D., Metzl N., Millero F., Munro D.R., Murata A., Nabel J.E.M.S., Nakaoka S., Nojiri Y., O'Brien K., Olsen A., Ono T., Pérez F.F., Pfeil B., Pierrot D., Poulter B., Rehder G., Rödenbeck C., Saito S., Schuster U., Schwinger J., Séférian R., Steinhoff T., Stocker B.D., Sutton A.J., Takahashi T., Tilbrook B., van der Laan-Luijkx I.T., van der Werf G.R., van Heuven S., Vandemark D., Viovy N., Wiltshire A., Zaehle S., and Zeng N. (2015) Global Carbon Budget 2015, Earth Syst. Sci. Data, vol. 7, pp. 349-396.

Maksyutov S., Takagi H., Valsala V.K., Saito M., Oda T., Saeki T., Belikov D.A., Saito R., Ito A., Yoshida Y., Morino I., Uchino O., Andres R.J., and Yokota T. (2013) Regional CO2 flux estimates for 2009-2010 based on GOSAT and ground-based CO2 observations, Atmospheric Chemistry and Physics, vol. 13, is. 18, pp. 9351-9373.

Neale R.B., J.Richter, S.Park, P.H.Lauritzen, S.J.Vavrus, Ph.J.Rasch, and Z.Minghua (2013) The mean climate of the community atmosphere model (CAM4) in forced SST and fully coupled experiments, *Journal of Climate*, 26, 5150–5168.

NIR 2012, Poland's National Inventory Report 2012, KOBIZE, Warsaw, 2012, 358 p., Available online at: http://unfccc.int/national_reports.

Oda T., and Maksyutov S. (2011) A very high-resolution (1 km×1 km) global fossil fuel CO_2 emission inventory derived using a point source database and satellite observations of nighttime lights, Atmos. Chem. Phys., 11, 543-556.

Oda T., Ott L., Topylko P., Halushchak M., Horabik-Pyzel J., Bun R., Lesiv M., and Danylo O. (2017) Assessing uncertainties associated with a global high-resolution fossil fuel CO_2 emission dataset (this issue).

Olivier J.G.J., Van Aardenne J.A., Dentener F., Pagliari V., Ganzeveld L.N., and Peters J.A. (2005). Recent trends in global greenhouse gas emissions: regional trends 1970-2000 and spatial distribution of key sources in 2000, Journal of Integrative Environment Science, vol. 2 (2-3), pp. 81-99.

Ometto J.P. (2015) Uncertainties in Greenhouse Gas Inventories - Expanding Our Perspective, Ometto, J.P., Bun, R., Jonas, M., Nahorski, Z. (Eds.), Springer, 239 p.

Pétron G., Tans P., Frost G., Chao D., and Trainer M. (2008) High-resolution emissions of CO_2 from power generation in the USA, J. Geophys. Res., vol. 113, is. G4, pp. 1-9.

Puliafito S.E., Allende D., Pinto S., and Castesana P. (2015) High resolution inventory of GHG emissions of the road transport sector in Argentina, Atmospheric Environment, vol. 101, pp. 303-311.

Raupach M.R., Rayner P.J., and Paget M. (2010) Regional variations in spatial structure of nightlights, population density and fossil-fuel CO_2 emissions, Energy Policy, vol. 38, pp. 4756–4764.

Rayner P. J., Raupach M.R., Paget M., Peylin P., and Koffi E. (2010) A new global gridded data set of CO_2 emissions from fossil fuel combustion: Methodology and evaluation, J. Geophys. Res., 115, D19306, 11 p.

Spencer Th., Colombier M., Wang X., Sartor O., Waisman H. (2016) Chinese emissions peak: Not when, but how, IDDRI Working Papers, Is. 7, 22 p.

Striamets O., Lyubinsky B., Charkovska N., Stryamets S., Bun R. (2014) Geodistributed analysis of forest phytomass: Subcarpathian voivodeship as a case study, Econtechmod, vol. 3, is. 1, pp. 95-104.

Topylko P., Halushchak M., Bun R., Oda T., Lesiv M., Danylo O., and Jonas M. (2017) Spatial greenhouse gas inventory and uncertainty analysis: A case study of electricity generation and fossil fuels processing (this issue).

Turner A.J., Jacob D.J., Wecht K.J., Maasakkers J.D., Lundgren E., Andrews A.E., Biraud S.C., Boesch H., Bowman K.W., Deutscher N.M., Dubey M.K., Griffith D.W.T., Hase F., Kuze A., Notholt J., Ohyama H., Parker R.J., Payne V.H., Sussmann R., Sweeney C., Velazco V.A., Warneke T., Wennberg P.O., and Wunch D. (2015) Estimating global and North American methane emissions with high spatial resolution using GOSAT satellite data, Atmospheric Chemistry and Physics, vol. 15, is. 12, pp. 7049-7069.

Valakh M., Bun R., Halushchak M., Danylo O. (2015) Spatial analysis of greenhouse gas emissions from linear objects: the transport sector of Subcarpathian voivodeship, Modeling and Information Technologies, vol. 74, pp. 82-89.

Verstraete J. (2014) Solving the map overlay problem with a fuzzy approach, Climatic Change, 2014, 124(3), 591-604.

Verstraete J. (2017) An artificial intelligent approach to spatial disaggregation: Analysis and performance (this issue).

White Th. (2011) Greenhouse Gas Inventories: Dealing With Uncertainty, White Th., Jonas M., Nahorski Z., Nilsson S., Eds., Springer, 343 p.